2020 2nd International Conference on Smart Power & Internet Energy Systems

20V HV Energy Harvesting Circuit with ACC/CV Mode and MPPT Control for a 5 W Solar Panel

Tzung-Je Lee*, *Senior Member, IEEE*
Department of Computer Science and Information Engineering
Cheng Shiu University
Kaohsiung, Taiwan 83347
tjlee@gcloud.csu.edu.tw

Po-Kai Su
Department of Electrical Engineering
National Sun Yat-Sen University
Kaohsiung, Taiwan 80424
pksu1207@vlsi.ee.nsysu.edu.tw

Chua-Chin Wang, *Senior Member, IEEE*
Department of Electrical Engineering
National Sun Yat-Sen University
Kaohsiung, Taiwan 80424
ccwang@ee.nsysu.edu.tw

***Abstract*—A HV energy harvesting circuit with ACC/CV mode and MPPT control is proposed for a 20 V/5 W solar panel. By considering the CC/CV charging process of the Li-ion battery and the changing maximum power point of the solar panel, the adaptive constant current (ACC) mode with PWM and MPPT control is utilized to improving the efficiency when the light source is not strong and the battery is not full. While the battery reaches full-charged, the constant voltage (CV) mode is used to prevent the damage to the Li-ion battery. The proposed design is implemented using TSMC 0.5 um UHV process. Based on the simulation results, the circuit achieves the tracking efficiency of 98% for the photocurrent from 0.1 A to 0.3 A.**

Keywords*—*energy harvest, MPPT, photovoltaic, ACC, CV

I. INTRODUCTION

Due to the applications of the wireless sensors [1], modern mobile devices [2], IoT (Internet of Things) [3], wireless sensor networks (WSN) [4], and roof-integrated PV (photovoltaic) systems [5], PV energy harvesting becomes an attractive technique because the solar energy possesses highest power density [6]. A 5 W PV panel with voltage ranging from 10 to 20V is widely used in the applications of medical equipment and air monitoring systems [7]. In order to improving the efficiency of the PV energy harvesting, various MPPT (Maximum power point tracking) techniques are presented in the prior works [1]-[11]. The incremental conductance method [8], the neural network and the fuzzy logic control method [9] compute the power and then trace the MPP (Maximum power point) using plenty of digital logic circuits, which needs the ADC and MCU. It results in a long tracking procedure and great cost. The analog power calculation method [10] and the perturb & observe (P&O) method (also called hill-climbing method) [5], [6], [11] to achieve fast tracking and reduce the system cost by sensing the output current proportional to the output power and then determining the MPP. The tracking speed is further improved by using the sectored hill-climbing method [1], which analyzes and stores the features of the solar panel with an embedded resistor array to obtain the MPP. This method is a customized design to the specific solar panel. Besides, these methods require complex control circuits. The fractional open circuit voltage (FOCV) method uses simple control circuits to sense the open circuit voltage and detect the MPPT [3], [4]. However, the precision is sacrificed.

In this work, a 5 W solar panel with 10~20V voltage is used as the energy source and a Li-ion battery of 3.6 V to 4.2 V is used as the energy storing device. By using the MPPT of P&O method, the adaptive constant current (ACC) mode with PWM control according to the output current of the solar panel is proposed. Moreover, the constant voltage (CV) mode is utilized when the li-ion battery reaches the full-charged for protect the Li-ion battery. The proposed design is carried out using TSMC 0.5 um UHV process. The simulation results show that the peak MPPT tracking efficiency is 98% with the power throughput of 5 W and the switching frequency of 1 MHz.

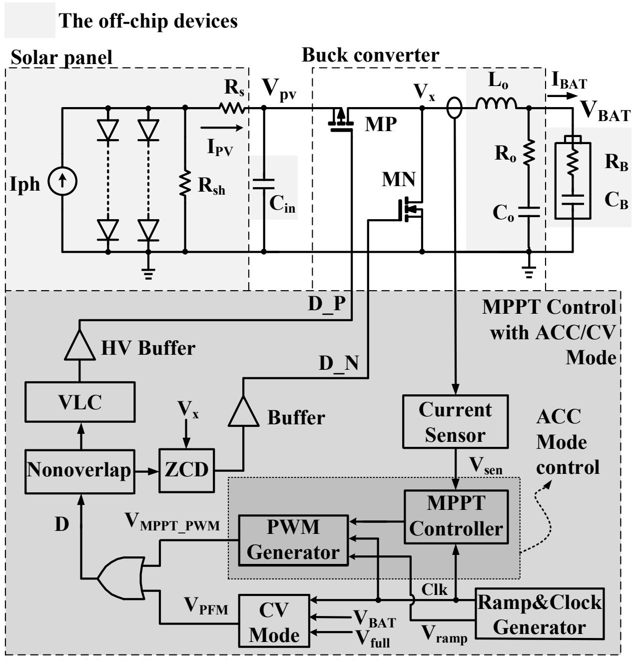

Fig. 1 The block diagram of the proposed design.

II. THE PROPOSED HV ENERGY HARVESTING CIRCUIT WITH ACC/CV MODE AND MPPT CONTROL

Fig. 1 shows the block diagram of the proposed design, which includes a 5 W solar panel energy source, a Li-ion battery load with voltage from 3.6 V to 4.2 V, a Buck converter as the energy harvesting circuit and a MPPT Control circuit with ACC and CV modes. The 2-D model is used to simulate the solar panel of voltage from 10 V to 20 V. I_{PH} refers to the generated photocurrent, which varies according to the light source strength. R_s and R_{sh} are the parasitic series and parallel resistors, respectively. The cascode diodes denotes the solar panel composed of cascode PV cells. I_{PV} and V_{PV} are the output current and output voltage of the solar panel, respectively. The buck converter comprises the HV 20 V MOS transistors, MP and MN, the inductor, L_o, and the capacitor, C_o. Notably, R_o is the effective resistor of C_o.

The MPPT Control circuit uses a Current Sensor to sense the output battery current, I_{BAT}. Besides, a Ramp&Clock Generator generates the required switching signal, Clk, and the ramp signal, V_{ramp}. The MPPT Controller and the PWM

*Prof. T.-J. Lee is the contact author. (Email: tjlee@gcloud.csu.edu.tw)

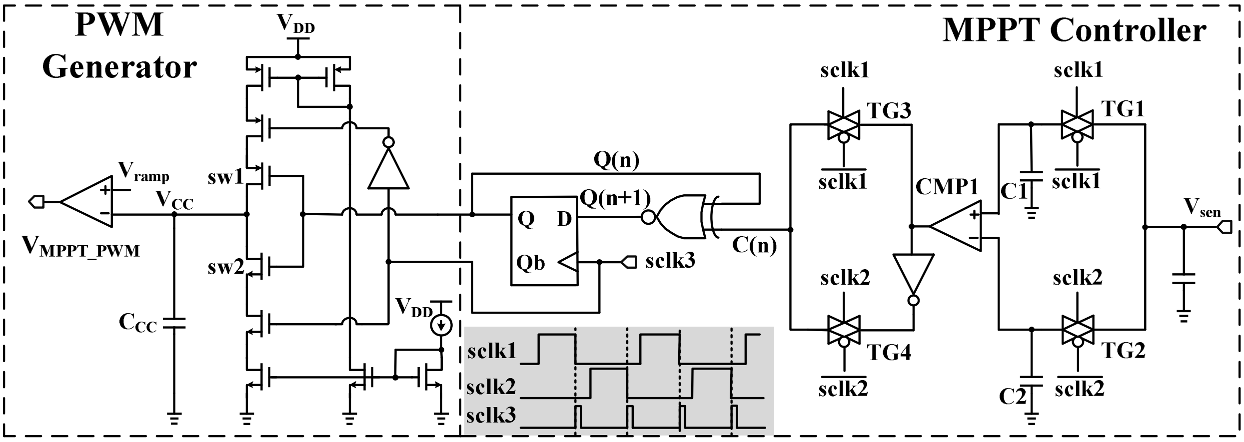

Fig. 2 Schematic of the proposed ACC Mode control with MPPT Controller and the PWM Generator.

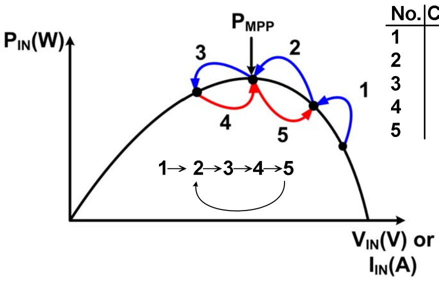

No.	C(n)	Q(n)	Q(n+1)
1	1	1	1
2	1	1	1
3	0	1	0
4	1	0	0
5	0	0	1

Fig. 3 The MPPT tracking process.

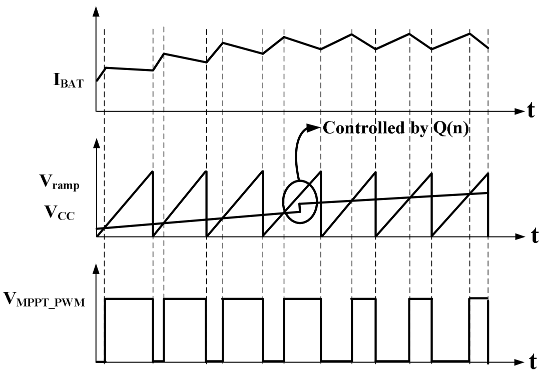

Fig. 4 The waveforms of I_{BAT}, V_{ramp}, VCC and V_{MPPT_PWM} during the

Generator are employed for the ACC Mode control to charging the Li-ion battery with the constant current according to the light strength. A CV Mode control circuit adjusts a small output current based on PFM to charge and protect the Li-ion battery. Besides, a Nonoverlap circuit is used to avoid the unwanted large instant conduction current through MP and MN. A ZCD (Zero-current detector) is to turn MN off when an inverse current is detected. The low-side driving signal, D_N, is then obtained by a Buffer. A VLC (Voltage level converter) and a HV Buffer are used to generate the driving signal, D_P, for the high-side transistor, MP.

A. ACC mode charging with PWM and MPPT control

Fig. 2 reveals the schematic of the proposed ACC Mode control with the MPPT Controller and the PWM Generator [12]. The sensed signal, V_{sen}, is sampled successively by the transmission gates, TG1 and TG2. The sampled signals are then compared by the comparator, CMP1, to determine the operating power point. Referring to Fig. 3, the power point is adjusted by control signals, C(n), Q(n), and Q(n+1), which are generated by the XNOR gate and the DFF. C(n) of logic 1 refers to the current increased. Q(n) and Q(n+1) denote the changing direction of VCC in the last and the present cycle, respectively. Q(n) of logic 1 refers to the rising of VCC in the last cycle. Thus, the MPPT tracking process is achieved by repeating the loop composed of the paths 2, 3, 4 , and 5, as shown in Fig. 3. Because the current is proportional to the power of the solar panel and the variation of I_{BAT} at each cycle is very small, the MPPT is achieved. Moreover, Q(n) is utilized to control the switches, sw1 and sw2, to determine that the node V_{CC} is charged or discharged. Referring to Fig. 4, the MPPT control signal, V_{MPPT_PWM}, is then generated and is used to adjust the output current, I_{BAT}, according to V_{CC} and V_{ramp}. Notably, sclk1 and sclk2 are the sampling signals. Besides, sclk3 is the triggered signal of the DFF.

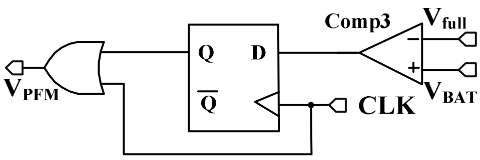

Fig. 5 The Schematic of the CV Mode control circuit

B. CV Mode control with PFM

The CV Mode control circuit is showed in Fig. 5. With the comparator Comp3, V_{BAT} is compared to the reference voltage, V_{full}, which is 4.2 V to indicate that the Li-ion battery is full-charged. When V_{BAT} is greater than V_{full}, the output of the DFF is logic 1 such that the output signal, V_{PFM}, keeps at logic 1. For $V_{BAT} < V_{full}$, the output of the DFF is logic 0 and V_{PFM} is coupled to the clock signal, CLK, by the OR gate. The waveforms are illustrated in Fig. 6.

C. Current Sensor and ZCD

The Current Sensor is revealed in Fig. 7. By using the current mirrors of the transistors, M1 and MP, with the ratio of the feature size equaling to 1/K, the sensed internal current through MR would be $\frac{I_{BAT}}{K} - I_{BIAS}$, because the current through M1 and M2 are $\frac{I_{BAT}}{K}$ and I_{BIAS}, respectively. The output voltage, V_{sen}, is then expressed by the following equation. If $I_{BIAS} \ll \frac{I_{BAT}}{K}$, V_{sen} would be linearly proportional to the battery current, I_{BAT}.

$$V_{sen} = \left(\frac{I_{BAT}}{K} - I_{BIAS}\right) \cdot R_{sen} \quad (1)$$

D. Current Sensor and ZCD

Fig. 8 shows the schematic of the ZCD. When Vx is pulled to 0V, the DFF is reset and D_N becomes 0 V to turn MN off. When Vx > 0V, D_N is coupled to the signal, VN, provided by the Nonoverlap circuit for normal operation.

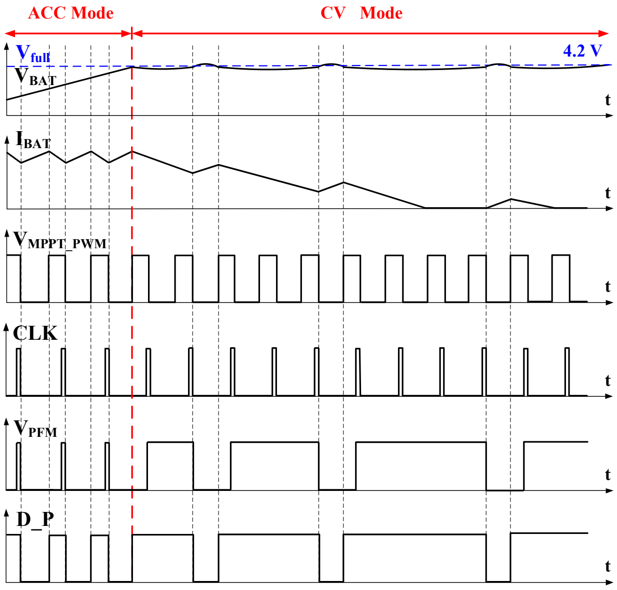

Fig. 6 The waveforms in the ACC mode and CV mode control

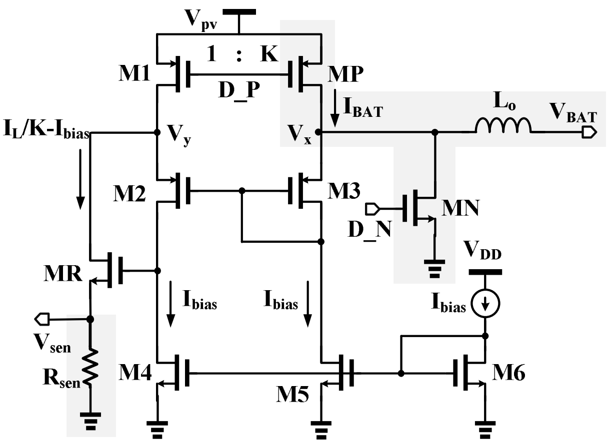

Fig. 7 Schematic of the Current Sensor.

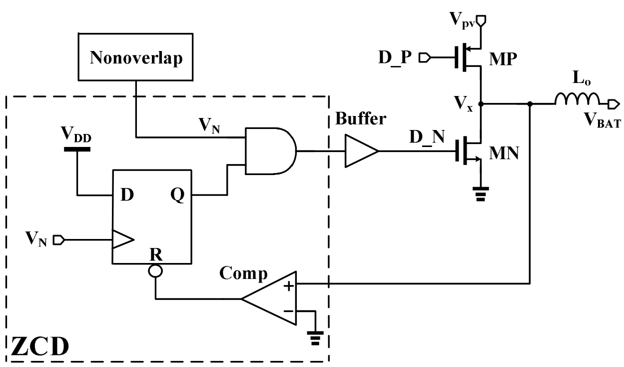

Fig. 8 Schematic of the zero-current detector (ZCD).

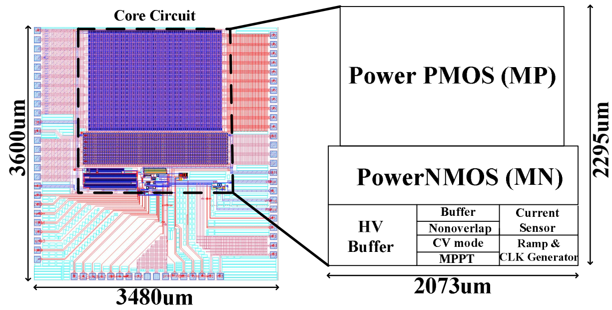

Fig. 9 Layout of the proposed design.

III. Implementation and Simulation Results

The proposed design is implemented using a typical 0.5 um UHV process. Fig. 9 shows the layout of the proposed design, where the area is 3600 × 3480 um^2. The core area is 2073 × 2295 um^2. Fig. 10 shows the simulated waveforms of the energy harvesting circuit in the charging process. With I_{PH} changing from 0.3 A to 0.1 A and then back to 0.1 A, the control signals, C(n), Q(n), and Q(n+1), varies according to the MPPT process, as shown in Fig. 3. Besides, the output current, I_{bat}, is tracking the MPP and the battery voltage, V_{bat}, is increased at the same time. When V_{bat} reaches 4.2 V, the energy harvesting circuit operates in the CV mode and the current, I_{BAT}, becomes very small to protect the Li-ion battery from over-charging. In this case, the circuit does not operates at MPPT because the efficiency of the solar panel is not the first priority. However, the PFM control is utilized to improve the efficiency of the buck converter at the light load.

Fig. 11 reveals the enlarged view of the simulated waveforms of the control signals in ACC mode. V_{MPPT_PWM} is generated by comparing V_{ramp} and V_{CC}, as shown in Fig. 2. The driving signal, D_P, is then coupled to V_{MPPT_PWM} based on the PWM control in ACC mode.

The simulated enlarged waveforms of the control signals of the CV mode is revealed in Fig. 12. The driving signal, D_P, is the result of the OR operation of V_{MPPT_PWM} and V_{PFM}. In the CV mode, I_{BAT} reduces gradually to protect the battery. Moreover, the worst case of the peak MPPT efficiency is simulated to be 98% among the different processes of TT, FF, SS and the temperature variation of 0°C, 25°C, and 75°C.

Table I summarizes the performance comparison with several prior works. The proposed design provides the maximum operating voltage and the maximum power throughput. The FOM (Figure of merit) is given by considering the input voltage and the peak MPPT efficiency. The proposed design possesses the best performance.

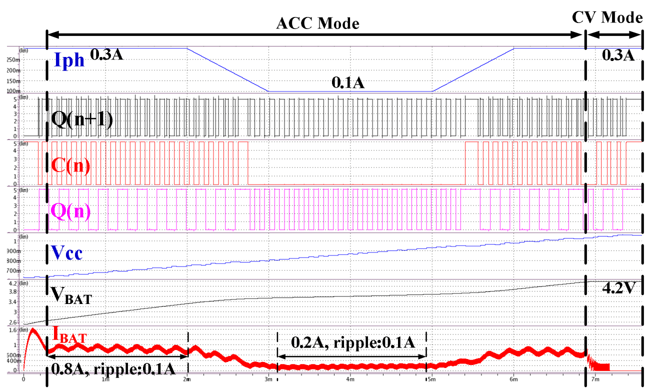

Fig. 10 Simulated waveforms in the charging process.

TABLE I. COMPARISONS WITH PRIOR WORKS

	[1]	[5]	[6]	[10]	This Work
Publication	ISSCC	TPE	VLSI-DAT	ISVLSI	SPIES
Year	2013	2013	2014	2015	2020
Technology	0.35μm	0.35μm	0.18μm	0.18μm	0.5μm
MPPT Method	Sectored Hill-Climbing	Quasi-P&O	P&O	P&O	P&O
Input voltage	0.5~2V	3.5~5.4V	0.5~1.1V	0.3-0.7V	10~20V
Output voltage	4.2V	NA	1.2~1.8V	NA	3.6~4.2V
Frequency (KHz)	500	530	NA	1000	1000
Power Throughput (W)	0.5	27	0.045	0.15	5
Peak MPPT Efficiency	99%	95%	90%	95%	98%
Power Consumption (mW)	3.4	0.56	NA	NA	20
Chip area (mm^2)	1.625	$0.45^{\#}$	1.43	$2.373^{\$}$	12.53
FOM*	1.98	5.13	0.99	0.665	19.6

Note: # The number indicates only the area of the control circuit of [5].
$ The number is only the core area.
* FOM = Max. input voltage × peak MPPT efficiency.

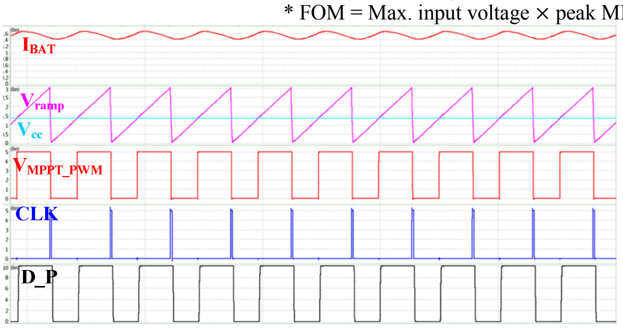

Fig. 11 Simulated waveforms in the ACC mode.

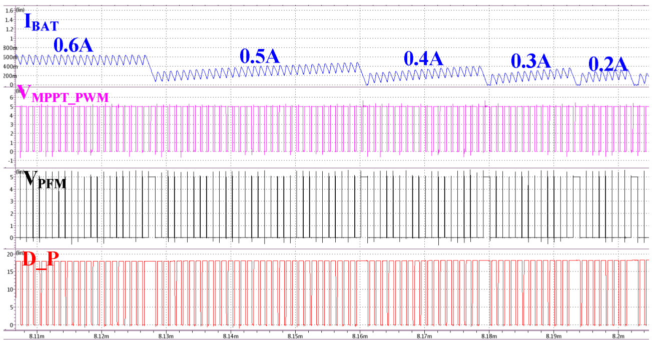

Fig. 12 Simulated waveform in the CV mode with I_{BAT} reduced from 0.6 A to 0.2 A.

IV. CONCLUSIONS

By using the MPPT and PWM control with ACC mode, the Li-ion battery is charged by the adaptive constant current based on the solar panel. The worst case of the peak MTTP efficiency is 98 % with the photocurrent from 0.1 A to 0.3 A among the various process and temperature simulation corners. Besides, the energy harvesting circuit enters the CV mode with PFM control when the voltage of Li-ion battery is close to 4.2 V to protect the battery from over-charging.

ACKNOWLEDGMENT

This investigation was partially supported by Ministry of Science and Technology, Taiwan, under grant MOST 108-2218-E-110-002-, MOST 108- 2218-E-110-011- and MOST 108-2221-E-230-008-. The authors would like to express our deepest appreciation to TSRI (Taiwan Semiconductor Research Institute) in NARL (Nation Applied Research Laboratories), Taiwan, for the assistance of chip fabrication.

REFERENCES

[1] T.-H. Tsai and K. Chen, "A 3.4mW Photovoltaic Energy-Harvesting Charger with Integrated Maximum Power Point Tracking and Battery Management," *in Proc. IEEE International Solid-State Circuits Conference Digest of Technical Papers*, pp. 72-73, Feb. 2013.

[2] W.-C. Liu, Y.-H. Wang and T.-H. Kuo, "An adaptive load-line tuning IC for photovoltaic module integrated mobile device with 470µs transient time, over 99% steady-state accuracy and 94% power conversion efficiency," *2013 IEEE International Solid-State Circuits Conference Digest of Technical Papers*, San Francisco, CA, 2013, pp. 70-71.

[3] T.-W. Hsu, H.-H. Wu, D.-L. Tsai and C.-L. Wei, "Photovoltaic Energy Harvester With Fractional Open-Circuit Voltage Based Maximum Power Point Tracking Circuit," in *IEEE Transactions on Circuits and Systems II: Express Briefs*, vol. 66, no. 2, pp. 257-261, Feb. 2019.

[4] D.-L. Tsai, H.-H. Wu and C.-L. Wei, "A low-power-consumption boost converter with maximum power tracking algorithm for indoor photovoltaic energy harvesting," *2017 IEEE Wireless Power Transfer Conference (WPTC)*, Taipei, 2017, pp. 1-3.

[5] R. Enne, M. Nikolic, and H. Zimmermann, "A Maximum Power-Point Tracker without Digital Signal Processing in 0.35µm CMOS for Automotive Applications," *in Proc. IEEE International Solid-State Circuits Conference Digest of Technical Papers*, pp. 102-103, Feb. 2012.

[6] S.-Y. Wang, H.-H. Wu and C.-L. Wei, "An integrated boost converter with maximum power point tracking for solar photovoltaic energy harvesting," *Technical Papers of 2014 International Symposium on VLSI Design, Automation and Test*, pp. 1-4, April. 2014.

[7] Datasheet: Poly-Crystalline Solar Panel. [on-line] Availabel: https://www. invensun.com/solar-panels/5w-solar-panel

[8] K. J. George, "Direct control method applied for improved incremental conductance mppt using SEPIC converter," *2014 International Conference on Green Computing Communication and Electrical Engineering (ICGCCEE)*, Coimbatore, 2014, pp. 1-6.

[9] V. V. Ramana and D. Jena, "Maximum power point tracking of PV array under non-uniform irradiance using artificial neural network," *2015 IEEE International Conference on Signal Processing, Informatics, Communication and Energy Systems (SPICES)*, Kozhikode, 2015, pp. 1-5.

[10] Y. Sugimoto, "The Solar Cells and the Battery Charger System Using the Fast and Precise Analog Maximum Power Point Tracking Circuits," *2015 IEEE Computer Society Annual Symposium on VLSI*, Montpellier, 2015, pp. 597-602.

[11] R. Enne, M. Nikolić and H. Zimmermann, "Dynamic Integrated MPP Tracker in 0.35 µm CMOS," in *IEEE Transactions on Power Electronics*, vol. 28, no. 6, pp. 2886-2894, June 2013.

[12] C.-C. Wang and G.-X. Liu, "A 1.5A 88.6% Li-ion Battery Charger Design using Pulse Swallow Technique in Light Load," *IEEE International Symposium on Circuits and Systems (ISCAS)*, pp. 1-4, Japan. 2019.